

Fluid Flow, Heat Transfer, Mixing Time and Inclusion Motion in Molten Steel Continuous Casting Tundish

Abdelbagi Mohamed Abdalla#1, Omer Ahmad Altohami #2

Mechanical Engineering Department, University of Kordofan, Sudan#1

Mechanical Engineering Department, University of Karary, Sudan#2

Abstract

The project of “Investigation to improve the secondary steel manufacturing process by adopting mathematical models“ was considered to contribute to the Strategic Steel Research in Sudan. The project was suggested as a close collaboration between Depart of mechanical engineering-University of Karray and the steel factories in Sudan. Steel cleanliness, which is aim of this project, is a focal point for Sudan young steel industry in order to maintain and strengthen their in-market and global competitiveness. The steady velocity and temperature fields were obtained by computationally solving, the Reynolds-Averaged Navier-Stokes (RANS) equations together with the energy equation, using the standard $k-\epsilon$ model of turbulence. These flow fields were then used to predict the inclusion removal by numerically solving the inclusion transport equation. For the mixing time characteristics transient solution was performed. The calculations were carried out using the commercial Computational Fluid Dynamics (CFD) software ANSYS-FLUENT 6.3.26.

The models results were compared and validated with experiments results, plant measurements and models reported in the open literature. The predicted inclusion separation fractions to the top surface (slag) were compared and well agreed with the results from [1] & [2]. Also a change of the inlet position is compared due to inclusion removal and mixing time. The inclusion removal efficiency increases with an increase in the distance between the inlet gate and outlet gates. The mixing time spent was longer by the far inlet gate, which was explained the better inclusion removal efficiency. Temperature distribution analysis was performed under steady state conditions for the constant heat fluxes from walls and from free surface of the tundish. The computed temperatures fields of steel melt in the tundish interior were showed approximately equalized temperature distribution, which was agreed well with the results from [1].

The project findings considered as first step and intended to be hopefully applied in the steel factories in Sudan.

Key words: Steel cleanliness; Tundish; Turbulent flow; Mixing time; Inclusion separation; Temperature distribution; Model validation; CFD.

1. Introduction

The tundish usage is to sustain the continuity of the casting process by keeping constant bath depth over the mold. The flow will be turbulent in the inlet and outlet regions and, in all likelihood, transitional in the bulk of the tundish system. There is practically no possibility to study metal movement on a real object, therefore the Mathematical modeling is an alternative approach for visualizing flow fields inside a tundish. Tundish flow field and associated inclusion removal process are strongly investigated with Computational Fluid Dynamics (CFD) models as well. Several studies can be found in literature [3] -[14]. The CFD techniques of today allow computing the fluid flow in tundish with the sufficient accuracy. This is established by a good agreement in flow fields predicted mathematically and measured by laser-optical method using water models [14]. In mathematical modeling, the turbulent Navier–Stokes equation is solved in a boundary fitted coordinate system to predict the velocity distributions. Analytical solution of 3D Navier–Stokes equation is not possible and so we have to go for numerical methods and for numerical solution of these equations a lot of commercial software packages like FLUENT, CFX, PHOENICS, FIDAP etc. have been marketed, and have allowed CFD to become an increasingly common tool for the non-experts [8]. Flow field is well described by steady-state numerical simulations using the Reynolds-Averaged Navier-Stokes (RANS) equations combined with the standard and realizable $k-\epsilon$ model to capture the critical effects of turbulent flow without having to resolve the actual small length and time scales of turbulent motion. On pre-calculated flow and turbulence field, the transport of disperse phase can be treated [8].

Steady 3-D flow of steel in the continuous casting tundish is simulated with finite-volume based software (fluent), the turbulence model used is the standard k- ϵ , Inclusion trajectories are calculated by integrating each local velocity, considering its drag and buoyancy forces. A “random walk” model is used to incorporate the effect of turbulent fluctuations on the particle motion. For the mixing time curves and its data, unsteady 3-D flow is used, to explore the fluid flow mechanism [2] [13].

Plant observations and final products mechanical properties tests in GIAD steel factory in Sudan have found that a serious quality problems, mainly brittleness of the final product (building bars), which may be as the results of many factors, including inclusion entrapment, slag entrapment in the steel melt and flow pattern in the tundish. As the results, these problems affect the productivity so as the improvement of the final product quality, which are permanent requirements concerning the continuous casting process, this was the motivation signal to conduct this research.

Sometimes the facilities to carry out experimental work may not (yet) available, in such case the CFD user must depend on among other on comparisons with high-quality data from closely related problems documented in the literature [15]. Therefore the validation and verification of the present models are carried out using results from experimental and modeling results from other researchers.

In the present work, fluid flow and inclusion separation as well as heat transfer analysis has been carried out on a six-strand tundish without use of any flow modifiers.

II. Model description & Pre-processing: geometry and grid generation

A. Model description

The geometry of the multi-strand Tundishes (which, is used to be a guide of the setting of CFD model for the use of the practical investigation in the targeted factories in Sudan) considered in the present study was the same as that used by Merder et al. [1] and Gupta and Dewan[2], which is a six-strand trough-type tundish designed for casting ingot employed for small cross-section rolled products, such as wire, rods, etc. Symmetry relative to the transverse plane passing through the inlet of the tundish is depicted in fig. 1. The detailed constructional parameters are: $L_1 = 2785$ mm, $L_2 = 2700$ mm, $L_4 = 500$ mm, $L_5 = L_6 = 1000$ mm, $W_1 = 1040$ mm, $W_2 = 850$ mm, $W_3 = 640$ mm, $W_4 = 450$ mm and steel bath height $H = 740$ mm. The inlet and outlet dia- meters of the gate are taken as 66 mm and 14 mm, respectively [1] [2]. The following properties of liquid steel were taken: specific

density equal 7010 kg/m^3 , specific heat equal 821 J/kg.K , thermal conductivity 30.5 W/m.K , and viscosity 0.007 kg/m.s [1] [2].

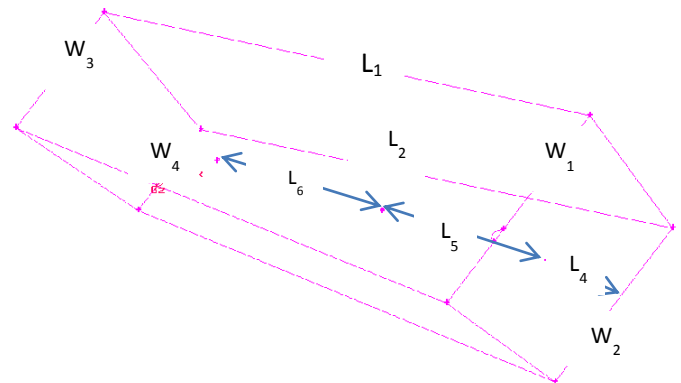


Fig.1. Schematic illustration of geometric and dimensions for the tundish (symmetric half of the tundish) employed in the numerical calculations.

B. Pre-processing: geometry and grid generation Symmetry assumed:

In the present work, symmetrical flow is presumed. Therefore Fig. 3 depicts a 3D half model of the tundish, which is also indicating boundary conditions.

For any CFD flow problem to be solved, Pre-processing is needed, to comprise the preparation of the geometry as well as dividing the domain of the flow into cells (grid). Pre-processing can be described as process of geometry and initial generation of the grid.

Pre-processing generates and initialize grid before the CFD solution process is commenced and taking place. Most CFD codes consist of an option to alter the grid based on the solution in progress, also recognized as solution adaptive-gridding. These grid refinement or coarsening, occur during the solution procedure and are clearly not part of pre-processing in CFD models. The pre-processor used in the present research is ANSYS-GAMBIT 2.4, which is the pre-processor for ANSYS-FLUENT[16].

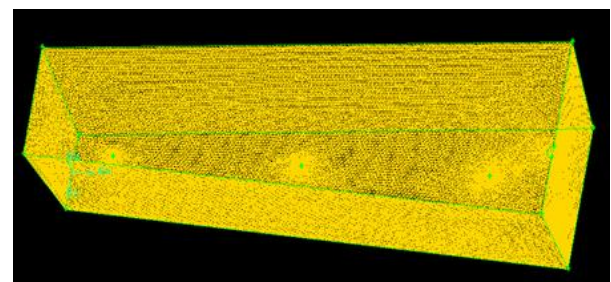


Fig.2 Illustrate the grid distribution in half of the tundish.

III. Quantitative indicators of tundish performance

To predict tundish performance, one should know the exact behavior of a tundish, what is happening inside it or how the fluid element is passing through it. This can be done by one of the two ways [22]:

a) By directly knowing how the fluid is passing through the tundish, ie. the complete velocity distribution of the fluid within the tundish.

b) By studying the flow characteristics of the system in terms of some defined parameters, which can give the idea of the flow behavior inside the tundish and its performance. ie. Quantification of performance in terms of some defined parameters like ‘mixing time characteristics curves’, ‘Residual ratio of inclusions’ etc. So the performance indicating parameters like ‘mixing time characteristics curves’ and ‘Inclusion separation’ are carried out in the present work.

IV. General Formulation of Flow Phenomena in Tundishes Fluid Flow

A 3D fluid flow model is founded on the continuity equation and Reynolds-averaged Navier-Stokes (RANS) equations for incompressible steel melt, conserving mass (one equation) and momentum (three equations) in addition to the energy equation at every point in a computational domain [4] [5] [8].

For most of the CFD problems, in addition to solve the above mentioned equations, in its original form, turbulence modeling is incorporated to capture the critical effects of turbulent flow without having to resolve the actual small length and time scales of turbulent motion[21] [23].

A. Governing Equations

The mathematical equations, which govern the computed fluid flow and inclusion separation are developed, and are solved by ANSYSFLUENT. The equations are represented in the Cartesian coordinate system and index notation. For a steady flow, these equations can be expressed as follows[4] [5]:

The continuity equation has the following form:

Continuity:

$$\frac{\partial}{\partial x_j} (\rho u_j) = 0 \quad (4.1)$$

The momentum conservation equation is to be expressed as follows:

$$\frac{\partial(\rho u_i)}{\partial t} + \frac{\partial(\rho u_i u_j)}{\partial x_{ij}} = -\frac{\partial P}{\partial x_i} + \frac{\partial}{\partial x_j} \left(\mu_{\text{eff}} \frac{\partial u_i}{\partial x_j} + \frac{\partial u_j}{\partial x_i} \right) + \rho g_i$$

(4.2)

μ_{eff} is the "effective viscosity" defined in the following equation[4] [5] [7] [10]:

$$\mu_{\text{eff}} = \mu + \mu_t \quad (4.3)$$

Here, i and j each represent the 3 coordinate directions, (x,y,z) and repeated indices imply summation. The effective viscosity, μ_{eff} , depends mainly on the turbulence parameters K and ϵ , found by solving two further transport equations.

The effect of thermal convection on the flow is accounted for with the Boussinesq approximation, which accounts for thermal buoyancy forces via the last term in Eq. 4.2

The effective viscosity appeared in Eqs. (4.2) has to be represented in terms of a turbulence model. In the present case, we have used the version of the K- ϵ model of Launder and Spalding [17] in which K is the specific turbulence energy and ϵ is the rate of turbulence energy dissipation. In many cases of turbulent flows, this model yields results close to experimental results, with limited computational outlays[1][4] [5] [8] [12] [23]

The associated relationships and the method of calculating K and ϵ are as follows [4] [5] [8] [12]:

Turbulent kinetic energy [5, 6, 8, 14]:

$$\frac{\partial(\rho k)}{\partial t} = \frac{\partial}{\partial x_i} \left[\left(\mu + \frac{\mu_t}{\sigma_k} \right) \frac{\partial k}{\partial x_i} \right] + G - \rho \epsilon \quad (4.4)$$

Dissipation rate of the turbulent kinetic energy:

$$\frac{\partial(\rho \epsilon)}{\partial t} = \frac{\partial}{\partial x_i} \left[\left(\mu + \frac{\mu_t}{\sigma_\epsilon} \right) \frac{\partial \epsilon}{\partial x_i} \right] + \frac{(C_{1\epsilon} \epsilon G - C_{2\epsilon} \rho \epsilon^2)}{k}$$

(4.5)

Where the generation of turbulence kinetic energy:

$$G = \mu_t \frac{\partial u_j}{\partial x_i} \left[\left(\frac{\partial u_i}{\partial x_j} + \frac{\partial u_j}{\partial x_i} \right) \right] \quad (4.6)$$

Empirical constants used in k- ϵ model [3] [4] [6] are as follow:

$C_{1\epsilon}$	$C_{2\epsilon}$	C_μ	σ_k	σ_ϵ
1.44	1.92	0.09	1	1.3

In this model, the effective viscosity is calculated from the relations:

$$(\text{effective viscosity}) = (\text{molecular viscosity}) + (\text{eddy viscosity})$$

(4.7)

Where:

$$\mu_t = C_\mu \rho \frac{K^2}{\epsilon} [4] [5] [8] [9] \quad (4.8)$$

The conservation equations (4.4) and (4.5) can be solved in order to calculate K and ϵ . Since these equations involve velocity terms, which are unknown at this stage this involves a lengthy iterative procedure.

In order to determine the distribution of temperature fields inside the tundish, mathematical model include the general equation of energy conservation for an incompressible Newtonian fluid, in the following form [1] [2] [16]:

$$\frac{\partial(\rho T)}{\partial t} + \frac{\partial(\rho u_j T)}{\partial x_j} = \frac{\partial}{\partial x_j} \left(\frac{k_{eff}}{c_p} \frac{\partial T}{\partial x_j} \right) \quad (4.9)$$

The effective thermal conductivity coefficient can be written as follows:

$$K_{eff} = \lambda + k_t \quad (4.10)$$

And the turbulent thermal conductivity is termed as:

$$K_t = \frac{c_p \mu_t}{Pr_t} \quad (4.11)$$

B. Tracer Dispersion

Because of the practical difficulties in obtaining and interpreting detailed knowledge of fluid flow pattern experimentally, an alternative approach to obtain the knowledge of how long different fluid elements remain in the tundish is obtained using a mixing time characteristics curves[1].

Tracer dispersion is an important tool in tundish characterization, used in the present work for steel grade change in order to estimate the mixing characteristics[1][2]. Tracer dispersion may be represented by

$$\frac{\partial}{\partial t} ((\rho c) + \frac{\partial}{\partial x_i} (\rho u_i c) + \frac{\partial}{\partial x_i} (\rho D_{eff} \frac{\partial c}{\partial x_i})) = 0 \quad (4.12)$$

In which D_{eff} is an effective diffusivity is the sum of the molecular diffusion coefficient and the turbulent diffusion coefficient

$$D_{eff} = D_m + D_t \quad (4.13)$$

The turbulent diffusion coefficient is determined from the following relationship (as summing that the turbulent Schmidt number is equal to unity)

$$\frac{\rho D_{eff}}{\mu_{eff}} \cong 1 \quad (4.14)$$

The presented system of equations was solved numerically by the control volume method in the three-dimensional (3D) domain.

A zero-flux condition is imposed on Eq. (4.12) on all solid surfaces, symmetry planes, and free surface.

C. Concentration (species) conservation equation

In steel process non-metallic inclusions enter the tundish as deoxidation products together with steel from the ladle or slag re-entering the melt or are the product of tundish lining erosion. In this research only the first type considered. In the numerical simulations thus only the inclusions come to the tundish with liquid steel, with the same initial velocities as steel, were tracked [11].

The transport of disperse phase can be treated on pre-calculated flow and turbulence field. There are two ways of modeling the discrete phase transport. The first approach is Langrangian particle tracking method, which is a full trajectory calculation. In this approach, each particle is treated separately and its trajectory is calculated by integrating local velocity. The differential equation, describing the motion of particles in the liquid, considers the different forces acting on particle, such as buoyancy force, drag force, added mass force and additional forces, but in this work only the drag-, buoyancy forces were considered, because the of negligible effect of other forces as reported in the literature [11] [20]. The second approach is the simple diffusion/convection approach. The particle concentration movement, due to turbulent transport and diffusion, is modeled by solving a transport equation, with the particle rise velocity as an extra convective component in the upward direction. When particle concentration is the dependent variable, the terminal rising velocity of particle is added to the velocity of the fluid[11].

In the present work inclusions trajectories were calculated using the Langrangian particle tracking method (discrete random walk model), which solves a transport equation for each inclusion as it travels through a previously calculated velocity field [11].

$$\frac{dl_{pi}}{dt} = u_{pi} \quad (4.15)$$

Where l_{pi} is inclusion location at any time in m. The inclusion velocity equation can be derived from the force balance. Here the drag force, F_d , and the gravitational force, F_g , are considered. Thus the total force acting on the inclusion, F , is represented by

$$F = m_p a_p = m_p \frac{du_p}{dt} = F_d + F_g = \frac{\pi}{8} d_p^2 \rho C_D (u_p - u)^2 - \frac{\pi}{6} d_p^3 g (\rho - \rho_p) \quad (4.16)$$

This yields the following: inclusion velocity equation

$$\frac{du_{pi}}{dt} = \frac{3}{4} \frac{1}{d_p} \frac{\rho}{\rho_p} C_D (u_{pi} - u_i)^2 - \frac{(\rho - \rho_p)}{\rho_p} g_i \quad (4.17)$$

where m_p is particle mass; a_p is particle acceleration rate; u is known liquid velocity; ρ is inclusion and liquid densities, $\text{kg}\cdot\text{m}^{-3}$; g is gravity acceleration, 9.8 m/s^2 along the vertical directions and zero at other directions; C_D is drag coefficient as a function of inclusion Reynolds number [11], given by

$$C_D = \frac{24}{Re_p} (1 + 0.186 Re_p^{0.653}) \quad (4.18)$$

The effect of the turbulent fluctuation on the motion of inclusions can be modeled crudely from a $\kappa\text{-}\epsilon$ flow field by adding a random velocity fluctuation at each step, whose magnitude varies with the local turbulent kinetic energy level.

Stochastic model [11]: The instantaneous fluid velocity can be represented by

$$U = \bar{u} + u' \quad (4.19)$$

$$u' = \xi \sqrt{u'^2} = \xi \sqrt{\frac{2k}{3}} \quad (4.20)$$

Where u is instantaneous fluid velocity, m/s; \bar{u} is average fluid phase velocity, m/s; u' is random velocity fluctuation, m/s; ξ – random number.

The separation rate of the particles from the tundish due to flotation is calculated with the formula:

$$\beta = \frac{N_{in} - N_{out}}{N_{in}} \times 100\% \quad (4.21)$$

Where: N_{in} is the number of particles at the inlet of the tundish and N_{out} is the number of particles at the outlet of the tundish.

D. Assumptions and boundary conditions

A symmetry boundary condition is given at a symmetry plane, which implies a zero gradient condition for all variables normal to the plane. Steel-slag interface is modeled as a frictionless wall. The Tundish walls were considered stationary (the so called “standard wall function”) for the velocity components and the turbulence quantities. Figure 3 illustrate different boundary conditions employed for the computations of the liquid steel flow through the tundish. The inlet velocity of liquid steel is equal to 0.9 m/s, which is equivalent to mass flow rate of 22.2 kg/s. The value of the turbulence intensity of entered flow was $I = 5\%$. The hydraulic diameter 0.04 m corresponds to the internal diameter of the shroud. For the heat transfer calculation, the boundary conditions include the incoming liquid steel temperature as 1850 K. The heat losses were supposed to be taking place through the walls, bottom and free surface of fluid in the tundish. The top surface heat loss was taken as $15,000 \text{ W/m}^2$ and from the tundish bottom

and walls the heat loss was taken as 2600 W/m^2 [1].

For the inclusion separation four different inclusion sizes ($20 \mu\text{m}$, $40 \mu\text{m}$, $60 \mu\text{m}$, $100 \mu\text{m}$) and density 5000 kg/m^3 were considered in the present study. The inclusions were inserted homogeneously through the inlet gate (520 inclusions per injection) and each inclusion’s trajectory was tracked until exited from the tundish outlets or it got trapped at the top wall [2] [12].

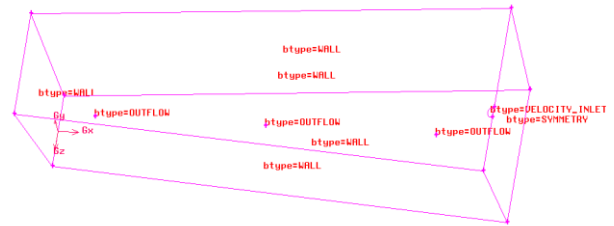


Fig.3 Geometry of the multi strand tundish showing different boundary conditions

Computer characteristics

The computer used of this work has the following characteristics:

Table 1: Computer characteristics

CPU	Intel ® Core™ i3 CPU M330 @ 2.13 GHz
Memory	4 GB of RAM
Mass storage service	500 GB
Operating System	Microsoft Windows 7 64 bits

V. Solution Procedure

Equations (4.1) to (4.11) (see section IV-A) represent the whole description of the problem. Because of the nonlinearity of the turbulent Navier-Stokes equations, numerical methods have to be used in order to obtain a solution. This model is simulated by the programs: ANSYS GAMBIT 2.4 and the commercial CFD software ANSYS-FLUENT 6.3.26.

Due to symmetry only a half of the tundish is simulated. One half of a tundish working space is reproduced by a TGrid computational grid with about 1.25 to 1.5 million of control volumes after some adaption steps on tundish configuration. For inlet and nozzle outlet ports smaller grid spacing is used by applying mesh refinement in order to visualize better the effects of velocity and turbulence gradients. The flow field in tundish is calculated using commercial CFD software

ANSYS-FLUENT 6.3.26 as stated above. The partial differential equations are solved with the help of the explained boundary conditions in IV (D) for all control volumes. To provide solution accuracy a QUICK scheme was implemented, to discretize the momentum, energy, turbulent kinetic energy and turbulent dissipation rate equations. SIMPLE algorithm was used to resolve the pressure-velocity coupling in the momentum equation. During iteration, the convergence was assumed to reach a point where the residuals are smaller than 10^{-3} for continuity, momentum, kinetic energy and kinetic energy dissipation rate, only for the energy is 10^{-6} .

VI. Results and Discussions

A. Mixing time characteristics

For assessing the present model, a validation study was carried out against the computational results reported by Merder et al. [1] and Dewan [2]. They generated mixing time characteristics curves of a bare six-strand trough-type tundish by casting two different grades of steel in a single sequence, for the evaluation of the transition zone during casting. In the present work the same procedure is followed, firstly a steel grade is casted by using unsteady casting process for some time (till steady flow), and then replaced by new grade (having the same physical properties) with mass fraction unity through the inlet, followed by generation of a characteristics plot for the new grade steel until its mass fraction became unity at the outlets and the average mass fraction of the new grade steel against the flow time for each outlet strand is studied. Figures (4a, b, c, d) compares the mixing time characteristics for three outlet strands from the present computations case 1 & Case 2 (In the present work a change of the position of the inlet of the tundish is considered, in case 1, the position of the inlet gate is, in the middle of the transverse plane of symmetry and in case 2, which is similar to the configuration of [1] [2], at 0.35W1 from left. Fig. 1) and those reported by Merder et al. and Dewan [1] [2]. A good agreement is observed between the three (Figure 4b, c, d). It can be read out from the curves in which period of the process (for each of the outlets) the steel grade being currently cast, as defined in terms of chemical composition is predominant [1].

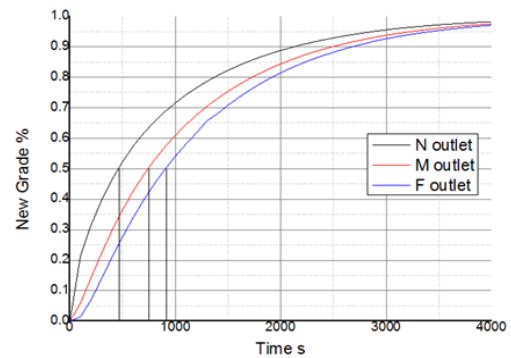


Fig. 4a (Case 1) mixing time characteristics of the present work {N (near).M (Middle), F (far) with respect to the inlet gate of the tundish }

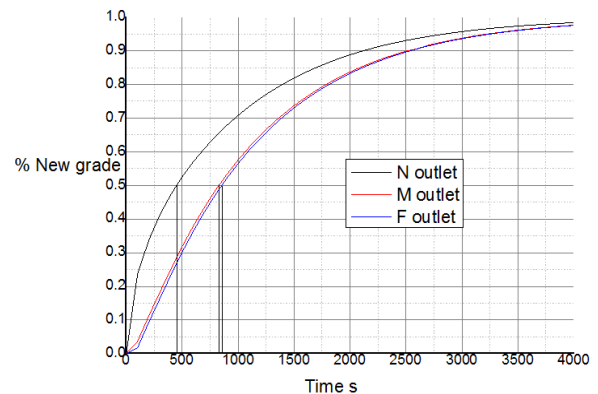


Fig. 4b(case2)Mixing time characteristics of the present work {N (near) M (Middle), F (far) with respect to the inlet gate of the tundish.

The developed characteristics shown in fig. 4b deliver an initial qualitative knowledge of the effect of the Tundish hydrodynamic conditions on the potentials of separating non-metallic inclusions. It can be visibly seen that the steel flowing through near outlet (fig.4b) has a short residence time, which is unfavorable for inclusions removal, but [18] reported that by using the conventional flow control devices like dams and weirs, this problem can be overcome, which will be attempted in future works.

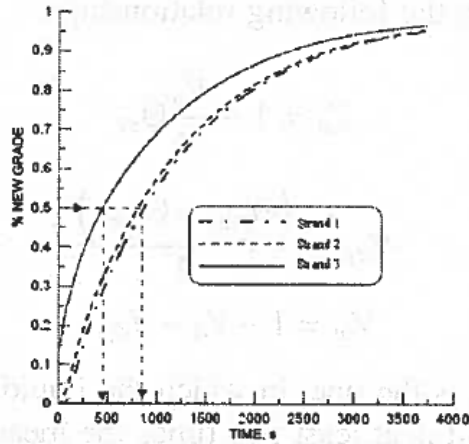


Fig. 4c Mixing time characteristics determined for three nozzles of the tundish [1]

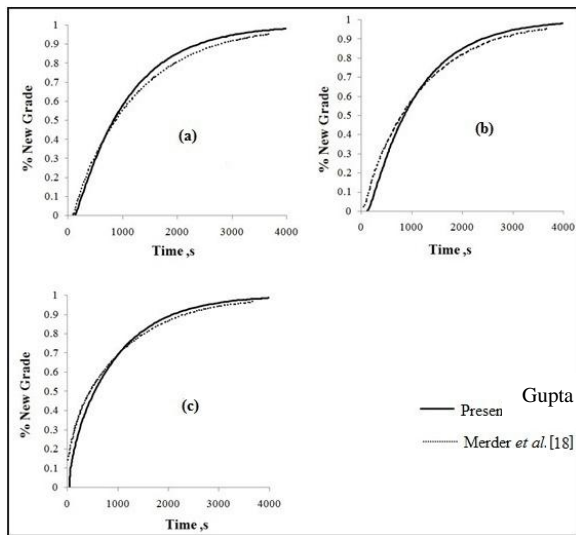


Fig. 4d A comparison of the mixing time characteristics reported by Merder et al and Dewan for the Far outlet (a), middle outlet (b) and near outlet (c) with those reported [2].

Velocity field.

Calculations were carried out for both steady and unsteady (transient) conditions. Unsteady calculations are only performed to determine the curves of steel mixing time characteristics. The solution of the model (steady state) with satisfactory convergence was obtained after performing many hundreds iteration by using pressure based solver- gradient option (Green Gauss node based) which is give a quick solution in comparison to Green Gauss cell based, when the grid type used is tetrahedral according to (FLUENT 6.3.26 user's manual) [16].

In the present work a change of the position of the inlet of the tundish is considered, in case1 (fig 5a, b, c), the position of the inlet gate is, in the middle of the transverse plane of symmetry and case2, which is the similar to the configuration of [1] [2], at 0.35W1 from left, (fig. 6a,b,c). Every case is represented in three control planes, for case1, indicated in (fig 5a,b,c). Fig.5a represent a plane crosses the tundish lengthwise passing through the inlet, while the plane in fig. 5b passes through the outlets and the plane in fig. 5c is the tundish symmetrical transverse plane. Fig. 6a, b, c are illustrated also in same sequence. The distribution of the velocity vectors in fig. 5c (through the inlet) indicate two distinct vortices of oppositely oriented rotation are observed. Such their arrangement should have a favorable effect on nonmetallic inclusions removal to the surface plane i.e. the slag. The flow pattern in case2 is similar to case one, the difference is in the inclusions removal, case 2 gave quite similar removal efficiency as [2] [12]. It's clear, the diagrams of this work show identical flow pattern as from [1]. The facet average velocity of the outlets is about 3.95m/s for the two cases.

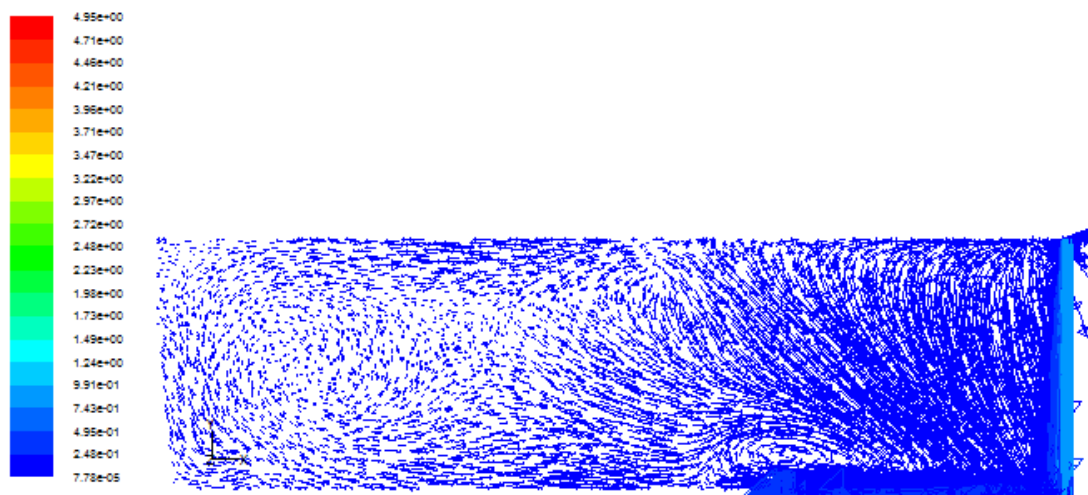


Fig.5a(Case 1) velocity vectors(colored by velocity magnitude) through a plane across the tundish lengthwise passing through the inlet

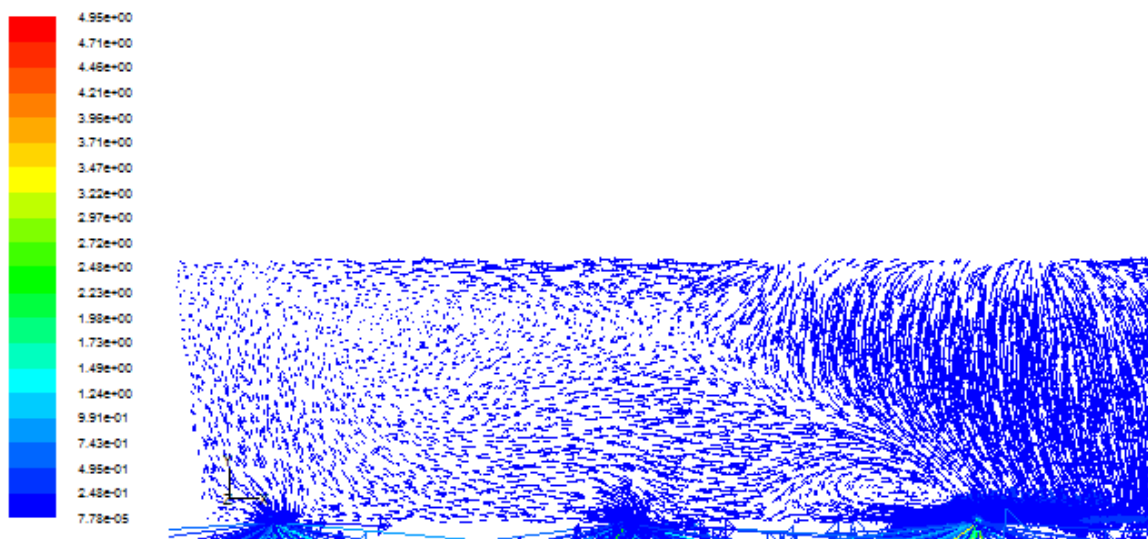


Fig.5b(Case 1) velocity field vectors through a plane across the tundish lengthwise passing through the outlets

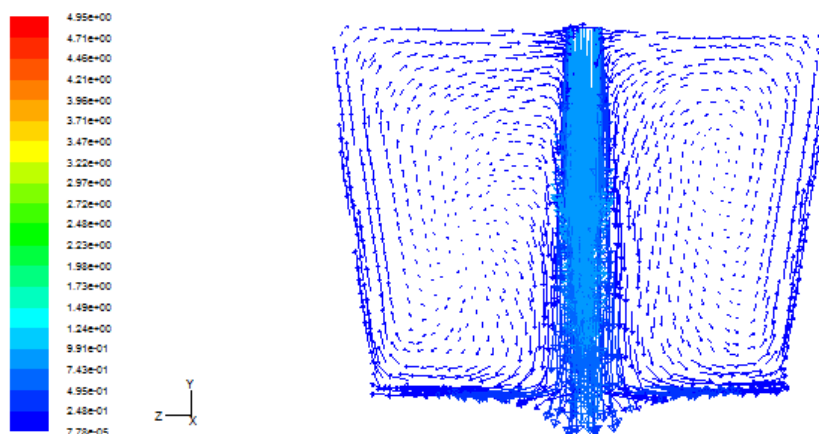


Fig.5c(case 1) velocity field vectors through the transverse symmetrical plane

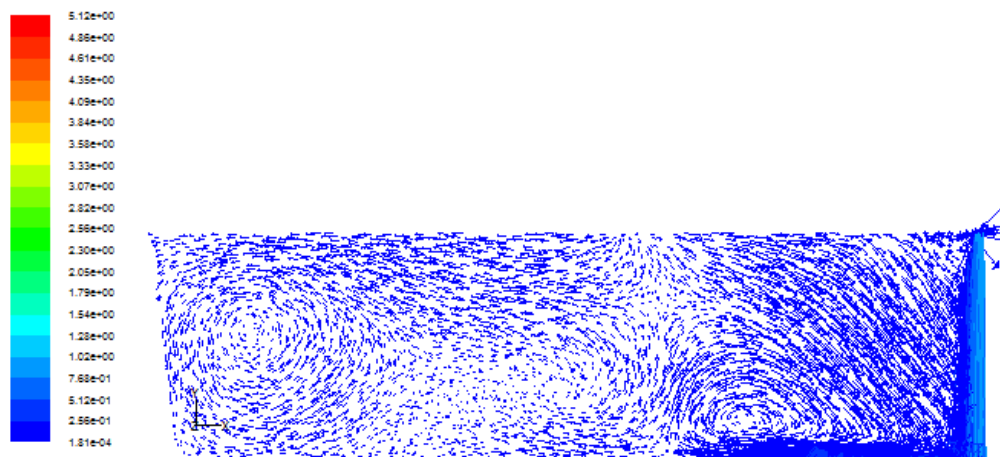


Fig.6a(Case 2) velocity field vectors through a plane across the tundish lengthwise passing through the inlet

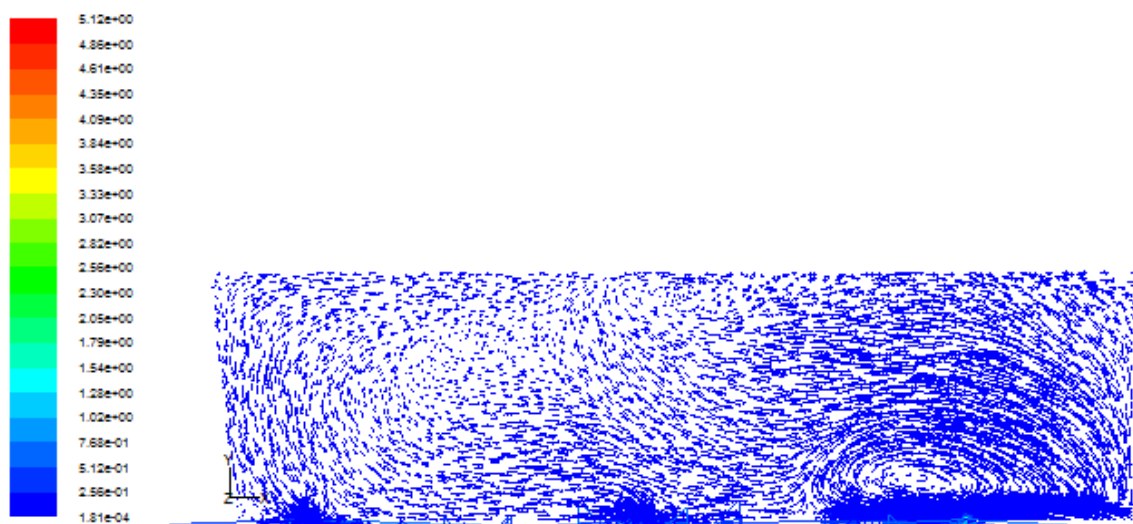


Fig.6b (CASE2) velocity field vectors through a plane across the tundish lengthwise passing through the outlets.

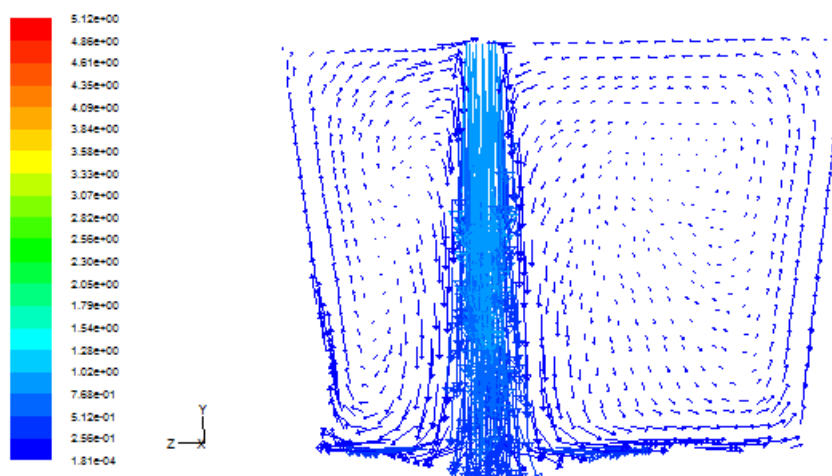


Fig.6c(Case 2) velocity field vectors through the transverse symmetrical plane

B. Temperature distribution

The computed fields of steel temperatures prevailing in the tundish interior have equalized distributions, which is illustrated in fig. 7a, b, c, d and the temperature differences at the outlets do not more than 10 K. the average temperature in the tundish interior is about 1844 K. that means it could be considered as isotherm. Also from fig. 7c, it can be seen, the far- and middle outlets have the same temperature which was agreed well with the results from [1]. Also a green region (region of lower temperature), can be seen at the top of the left portion of the surfaces of fig.7.a and 7.b, which is indicator of dead volume region. For decreasing the temperature difference between the strands, [19] reported that, in the case of multi-strand

casting situations, the heat loss may be different from strand to strand (this is approved in the present work as stated above), which may lead to some operational difficulties. Due to [19], it may be possible to even out the heat loss by appropriate baffling arrangements; for this reason, a precise knowledge of the flow field is quite desirable.



Fig. 7a Temperature distribution in the vertical plane through the inlet center



Fig. 7b Temperature distribution in the vertical plane through the outlets center

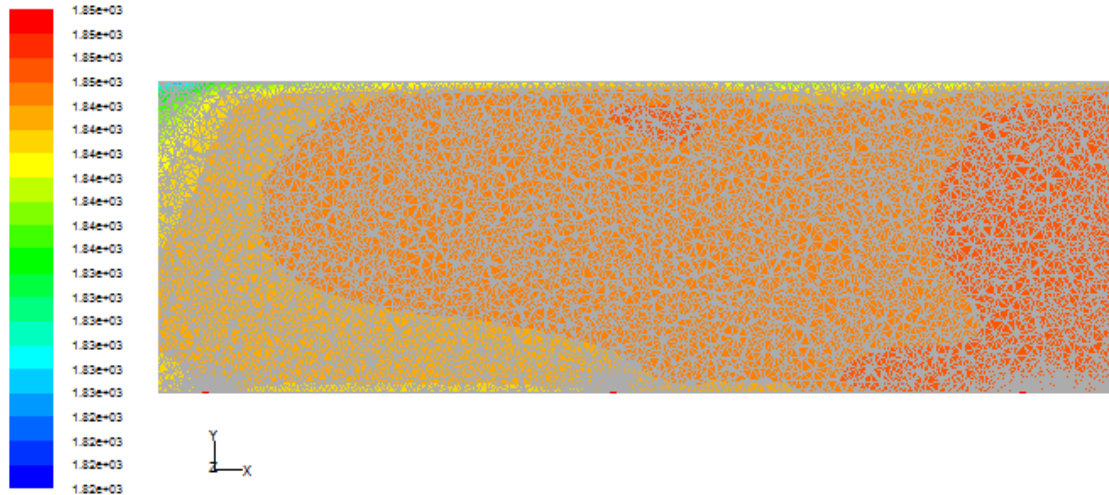


Fig. 7c Illustration of temperature distribution grid distribution in the vertical plane through the outlets centers.

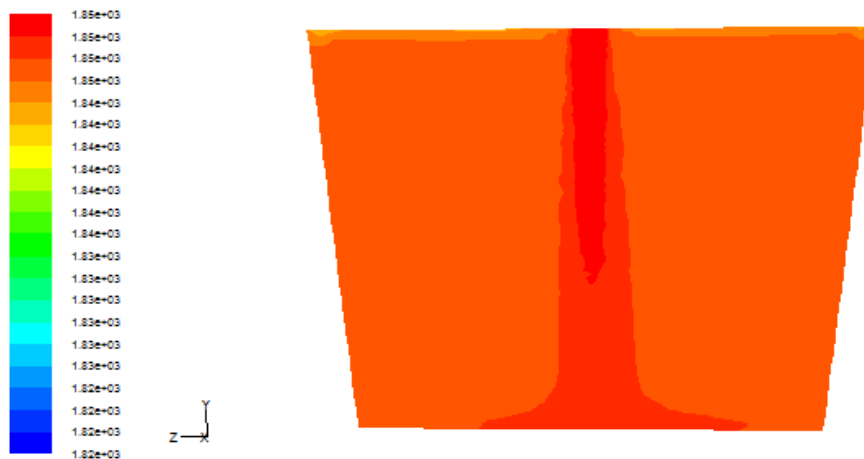


Fig. 7d Temperature distribution in the transverse symmetry plane through the inlet

A. Inclusion separation

A validation of the inclusion separation was performed by comparing the results of the present work with those reported by [1] [2] figure (8a) and(8b) respectively. [12] Has performed numerical simulations on inclusion separation in a single-strand tundish using the standard k-ε model and the trajectories of the inclusions inside the tundish were tracked by Langrangian particle tracking method, which is the same method used in this work. A good agreement between the present inclusion separation fractions predicted and those reported by (Mikki and Thomas) and (Gupta and Dewan) [2] [12] can be observed in Figure 8a(CASE2) and 8b respectively. As seen in fig 8a (CASE 1) the near inlet is unfavorable for inclusion removal in tundish.

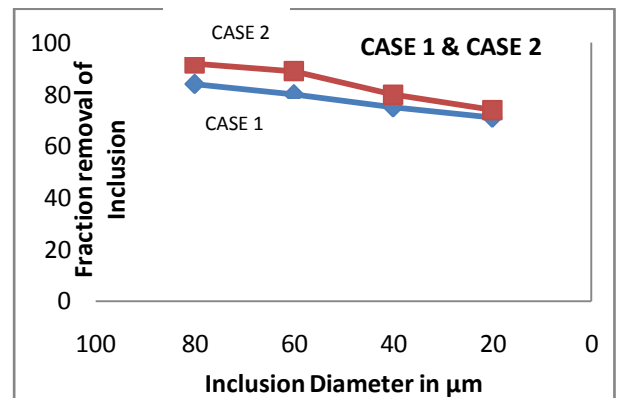


Fig.8a. Inclusion removal fraction of the present work

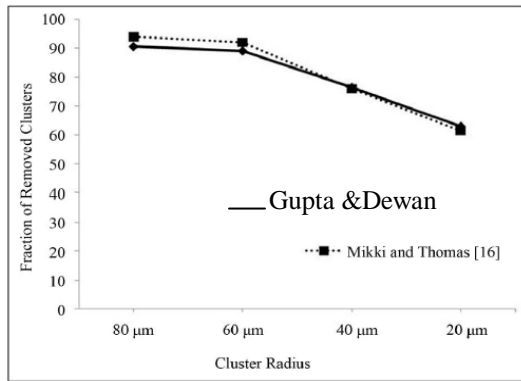


Fig. 8b. Inclusion fraction removal results reported by [2] [12]

It's clear from the diagrams above; an increase in particle removal rate into the top surface is occurred, as particle size increases, that is due to the effect of buoyancy force,

VII. Conclusion & Future work

In the presented work CFD numerical calculations, supported by experimental and modeled results from the open literature were performed, to simulate the flow of steel melt through the continuous casting tundish, non-metallic inclusions separation and temperature distribution. The base of the performed study was to model an industrial six-strand tundish configuration. The aim of the present study was to make a first step in the project mentioned in the abstract by comparing the model results from the present work with the experimental, plant measurement and models from [1] [2] [12] [13].

The numerical simulations of liquid steel flow in the tundish were performed using the commercial Computational Fluid Dynamics software ANSYS-FLUENT.

For assessing the present model, a validation study was performed against the computational results reported by Merder et al. [1] and Dewan [2] [13]. The comparison of the mixing time curves for the three outlet strands from the present computations (CASE 2) showed similar results as those reported by Merder et al. and Dewan [1] [2]. On pre-calculated flow field, the non-metallic inclusion removal in the investigated tundish of the present work was compared, validated and well agreed with the results from [1] [2] [12] [13]. Also a change of the inlet position was compared, for inclusion removal and mixing time. The inclusion separation fraction increases with an increase in the distance between the inlet gate and the outlet gates. The mixing time spent was longer by the far inlet gate, which explained the better inclusion removal efficiency. The temperature distribution indicated

approximately equalized temperature distribution, which agreed well with the results from [1].

Future work

The first recommendation would be to investigate possible use of flow regulators (weir, dams, flow inhibitors etc.) for every individual practice tundish investigated in steel factories in Sudan.

The second recommendation based on this research would be carried out to improve boundary condition describing inclusion separation at the steel-slag interface and to compute and evaluate the inclusion distribution at the tundish outlets.

References:

- [1] T. Merder, J. Jowza and A. Boguslawski, "The Analysis of the Conditions of Steel Flow in the Tundish Performed by a Numerical Methods," *Archives of Metallurgy and Materials*, pp. 933-953, Vol. 50, No. 4, 2005.
- [2] S. Gupta and A. Dewan, "Performance Optimization of a Six-Strand Tundish," *World Journal of Mechanics*, doi:10.4236/wjm.2013.33018 Published Online June 2013 (<http://www.scirp.org/journal/wjm>, pp. 184- 193, 3, 2013.
- [3] M. W. Czestochowa, " Numerical Modelling of Non-metallic Inclusion Separation in a Continuous Casting Tundish," *Computational Fluid Dynamics Technologies and Applications. InTech*, 2011.
- [4] M. Warzecha , T. Merder and B. P. Warzecha, "CFD modelling of non-metallic inclusions removal process in the T-type tundis," *Journal of Achievements in Materials and Manufacturing Engineering*, Vol. 55, ISSUE 2, December 2012.
- [5] Q. Hou and Y. You, "Comparison between standard and renormalization group k-ε models in numerical simulation of swirling flow tundish," *ISIJ international*, p. PP. 325 – 330, Vol. 45 (2005), No. 3.
- [6] . A. Kumar, D. Mazumdar and S. C. Koria, "Modeling of Fluid Flow and Residence Time Distribution in a Four-strand Tundish for Enhancing Inclusion Removal," *ISIJ International*, p. pp. 38–47, Vol. 48 (2008), No.1.
- [7] S. K. Mishra et al, "Numerical investigation of fluid flow and heat transfer in a multi-strand steelmaking tundish with closed strands," *International Journal of Engineering Science and Technology (IJEST)* 3.2 (2011).
- [8] . Chattopadhyay, Kinnor, Mihaiela Isac, and Roderick IL Guthrie "Physical and Mathematical Modelling of Steelmaking Tundish Operations: A Review of the Last Decade (1999–2009)," *ISIJ International*, p. pp. 331–348, Vol. 50 (2010), No. 3.
- [9] H. Bai and B. G. Thomas, "Two Phase Flow in Tundish Nozzles During Continuous Casting of Steel," in *Materials Processing in the Computer Age III*, V. Voller and H. Henein, eds., TMS Annual Meeting, Nashville, TN, Nashville, March 12-16, 2000.
- [10] M. Warzecha, T. Merder, P. Warzecha and G. Stradomski, "Experimental and Numerical Investigations on Non-metallic Inclusions Distribution in Billets Casted at a Multi-strand Continuous Casting Tundish," *ISIJ international* 53.11 (2013): 1983-1992.
- [11] L. Zhang, "Fluid flow and heat transfer and inclusion motion in molten steel continuous casting tundishes," in *Fifth International Conference on CFD in the Process Industries CSIRO, Melbourne, Australia, 13-15 December 2006*.
- [12] Y. Miki and B. G. Thomas, "Modeling of Inclusion Removal in a Tundish," *Metallurgical and Materials*

- Transactions B*, pp. 639-654, Vol. 30, No. 4, 1999.
- [13] A. Dewan and S. Gupta, "Comparison of Different Multi-Strand Tundishes," *RESEARCH 2013 (ICMER 2013) (2014)*: 135.
- [14] A. Braun, M. Warzecha and H. Pfeifer, "Numerical and Physical Modeling of Steel Flow in a Two-Strand Tundish for Different Casting Conditions," *Metallurgical and Materials Transactions B*, pp 549–559, June 2010, Volume 41, Issue 3.
- [15] H. K. Versteeg and W. Malalasekera., An Introduction to Computational Fluid Dynamics (The Finite Volume Method), Harlow: Pearson Education Limited, 2007.
- [16] "Fluent, A. N. S. Y. S. "Fluent 6.3 Documentation." *Fluent Inc., Lebanon, NH, 2006*.
- [17] B. E. Launder and D. B. Spalding, "Computer Methods App.," *Mech. Eng.*, 3(2), 269-289, 1974.
- [18] H. Turkoglu and B. Farouk, "Numerical computations of fluid flow and heat transfer in gas injected iron baths," *ISIJ International*, Vols. vol. 30, (11), pp.961-970, 1990.
- [19] Ilegbusi, O., and J. Szekely. "The Physical and Mathematical Modeling of Tundish Operations." 1989
- [20] R. Codina, Comparison of some finite element methods for solving the diffusion-convection-reaction equation, *Computer Methods in Applied Mechanics and Engineering*, Volume 156, Issues 1–4, 14 April 1998, Pages 185-210
- [21] Turbulence_Notes_Fluent-v6.3.06.pdf
www.southampton.ac.uk/~nwb/lectures/GoodPracticeCFD/Articles/Turbulence_Notes_Fluent-v6.3.06.pdf
- [22] S. K. Ray, "On the Application of Physical and Mathematical Modeling to Predict Tundish Performance," *PhD Thesis, Montreal, Canada, August, 2009*
- [23] A. Prabhaka, CFD Analysis of Static Pressure and Dynamic Pressure for NACA 4412, *International Journal of Engineering Trends and Technology (IJETT) - Volume4 Issue8- August, Page 3258 2013*